Applied Meteorology Unit (AMU)

Quarterly Report

Second Quarter FY-03

Contract NAS10-01052

30 April 2003

Distribution

NASA HQ/M/F. Gregory
NASA KSC/AA/R. Bridges
NASA KSC/MK/W. Hale
NASA KSC/PH/ M. Wetmore
NASA KSC/PH/E. Mango
NASA KSC/PH/M. Leinbach
NASA KSC/PH/S. Minute
NASA KSC/PH-A/J. Guidi
NASA KSC/YA/J. Heald
NASA KSC/YA-C/D. Bartine
NASA KSC/YA-D/H. Delgado
NASA KSC/YA-D/J. Madura
NASA KSC/YA-D/F. Merceret
NASA JSC/MA/R. Dittemore
NASA JSC/MS2/C. Boykin
NASA JSC/ZS8/F. Brody
NASA JSC/ZS8/R. Lafosse
NASA MSFC/ED03/S. Pearson
NASA MSFC/ED41/W. Vaughan
NASA MSFC/ED44/D. Johnson
NASA MSFC/ED44/B. Roberts
NASA MSFC/ED44/S. Deaton
NASA MSFC/MP01/A. McCool
NASA MSFC/MP71/S. Glover
45 WS/CC/N. Wyse
45 WS/DO/P. Broll
45 WS/DOR/S. Cabosky
45 WS/DOR/J. Moffitt
45 WS/DOR/J. Sardonia
45 WS/DOR/J. Tumbiolo
45 WS/DOR/ K. Winters
45 WS/DOR/J. Weems
45 WS/SY/ T. McNamara
45 WS/SYR/W. Roeder
45 WS/SYA/B. Boyd
45 MXG/CC/B. Presley

45 MXG/LGP/R. Fore
45 SW/SESL/D. Berlinrut
CSR 4140/H. Herring
CSR 7000/M. Maier
SMC/CWP/G. Deibner
SMC/CWP/T. Knox
SMC/CWP/R. Bailey
SMC/CWP (PRC)/P. Conant
Hq AFSPC/DORW/R. Thomas
Hq AFWA/CC/C. French
Hq AFWA/DNX/E. Bensman
Hq AFWA/DN/N. Feldman
Hq USAF/XOW/H. Tileston
NOAA "W/NP"/L. Uccellini
NOAA/OAR/SSMC-I/J. Golden
NOAA/NWS/OST12/SSMC2/J. McQueen
NOAA Office of Military Affairs/M. Weadon
NWS Melbourne/B. Hagemeyer
NWS Southern Region HQ/"W/SRH"/X. W. Proenza
NWS Southern Region HQ/"W/SR3"/D. Smith
NWS/"W/OSD5"/B. Saffle
NSSL/D. Forsyth
FSU Department of Meteorology/P. Ray
NCAR/J. Wilson
NCAR/Y. H. Kuo
30 WS/SY/C. Crosiar
30 WS/CC/P. Boerlage
30 SW/XP/J. Hetrick
NOAA/ERL/FSL/J. McGinley
Office of the Federal Coordinator for Meteorological
    Services and Supporting Research
Boeing Houston/S. Gonzalez
Aerospace Corp/T. Adang
Yankee Environmental Systems, Inc./B. Bauman
Lockheed Martin Mission Systems/T. Wilfong
ACTA, Inc./B. Parks
ENSCO, Inc./E. Lambert

EXECUTIVE SUMMARY

This report summarizes the Applied Meteorology Unit (AMU) activities for the Second Quarter of Fiscal Year 2003 (January − March 2003). A detailed project schedule is included in the Appendix.

Task   Statistical Forecast Guidance for the Shuttle Landing Facility (SLF) Towers

Goal   Calculate climatologies and probabilities for the 10-minute peak winds at the SLF to aid in Flight Rule evaluation, and create a PC-based graphical user interface (GUI) to access the data.

Milestones   Task has been completed with the final report in review, and the GUI is now in operational use at the Spaceflight Meteorology Group (SMG).

Discussion   Chart of the SLF wind tower climatologies and probabilities were provided to SMG, but they may be awkward to manipulate and interpret in a fast-paced operational environment. A GUI was developed to allow quick access to the data. SMG was consulted on the design, which ensured that the end product would produce useful information easily in a readable format.

Task   Doppler miniSODAR™ System (DmSS) Evaluation

Goal   Compare data from the DmSS near SLC-37 to data from nearby towers to determine the quality of the DmSS data. Boeing is evaluating these data for their utility in analyzing and forecasting winds for the new Evolved Expendable Launch Vehicle during ground and launch operations.

Milestones   Continued acquisition and analysis of data from the DmSS and Towers 0006 and 0108.

Discussion   A 20-day average of wind profiles from the DmSS and Towers 0006 and 0108 indicate that the DmSS wind speeds tend to be lower at heights below 150 ft. An analysis of the wind speed time series during the Delta-IV launch countdown on 10 March 2003 suggests that DmSS wind speeds may be adversely affected by the diurnal cycle of solar heating. They correlated well with tower speeds during the day, but under-estimated the speeds during the night.

Task   Extend Automated Meteorological Profiling System (AMPS) Moisture Profiles

Goal   Evaluate the differences in moisture profiles between the AMPS and Meteorological Sounding System (MSS) and determine their impact on thunderstorm forecasting indices, which are critical for launch, landing, and ground operations and facilities warnings.

Milestones   Completed memorandum detailing the analysis of the 20 dual-sensor AMPS/MSS profiles taken in July and August 2002.

Discussion   There were no differences between the AMPS and MSS stability indices computed from warm-season data, although relative humidity (RH) profile differences indicated that AMPS would show the atmosphere to be more unstable. The AMU resolved this paradox by finding a weak temperature difference between AMPS and MSS that counteracts the RH differences.

Task   Verification of Numerical Weather Prediction Models

Goal   Develop an automated method that will verify specific weather phenomena in high-resolution models in order to improve upon traditional verification techniques. These models are used by Range Safety for toxic hazard predictions during launch, landing, and ground operations.

Milestones   Completed a draft final report describing the new Contour Error Map (CEM) method.

Discussion   The CEM is an automated method developed to identify the sea breeze in observed and model forecast wind fields. Results from the CEM compared well to a meteorological analysis of observed and model forecast sea-breeze locations over the Cape area. A phenomenological-based method like the CEM can save time and resources when verifying model forecasts, and can help improve the quality of verification results by focusing on a specific phenomenon.

Table of Contents

SPECIAL NOTICE TO READERS

Applied Meteorology Unit (AMU) Quarterly Reports are now available on the Wide World Web (WWW) at http://science.ksc.nasa.gov/amu/home.html.

The AMU Quarterly Reports are also available in electronic format via email. If you would like to be added to the email distribution list, please contact Ms. Winifred Lambert (321-853-8130, lambert.winifred@ensco.com). If your mailing information changes or if you would like to be removed from the distribution list, please notify Ms. Lambert or Dr. Francis Merceret (321-867-0818, Francis.J.Merceret@nasa.gov).

BACKGROUND

The AMU has been in operation since September 1991. Tasking is determined annually with reviews at least semi-annually. The progress being made in each task is discussed in this report with the primary AMU point of contact reflected on each task and/or subtask.

AMU ACCOMPLISHMENTS DURING THE PAST QUARTER

SHORT-TERM FORECAST IMPROVEMENT

EXTEND STATISTICAL FORECAST GUIDANCE FOR THE SLF TOWERS (MS. LAMBERT)

The peak winds near the surface are an important forecast element for both the Space Shuttle and Expendable Launch Vehicle (ELV) programs. As defined in the Launch Commit Criteria (LCC) and the Shuttle Flight Rules (FRs), each vehicle has certain peak wind thresholds that cannot be exceeded in order to ensure the safety of that vehicle during launch and landing operations. The 45th Weather Squadron (45 WS) and the Spaceflight Meteorology Group (SMG) indicate that peak winds are a challenging parameter to forecast. In Phase I of this task, climatologies and distributions of the 5-minute average and peak winds were created for the towers used in evaluating LCC and FRs. However, SMG uses a 10-minute peak as the standard for determining and verifying wind speed FRs. The goal of this phase of the task is to re-calculate the distributions and resulting probabilities of exceeding peak-wind thresholds using a 10- instead of 5-minute peak for the Shuttle Landing Facility (SLF) towers for all months. A tool was developed that can be used on a personal computer (PC) to display the desired information quickly and easily.

PC-Based Tool

Two products are available for SMG forecasters to access the climatology and probability values. The first is the Excel pivot charts and tables similar to those developed during Phase I (Lambert 2002). These displays are very flexible, allowing changes to the charts and tables with point-click-drag techniques. Axes can be switched, multiple variables can be represented on one axis, and specific curves can be temporarily removed from the display to facilitate closer examination of the remaining curves. Although they provide a useful visualization of the wind speed behavior with hour and direction, confident use of the pivot charts requires training and experience. Even with experience, the charts could still be difficult to manipulate and interpret in a fast-paced operational environment. The forecasters requested that a PC-based graphical user interface (GUI) be developed that would display the requested information quickly and in an easy-to-interpret format. Therefore, a PC-based GUI tool was developed to display the 5- and 10-minute peak wind speed climatologies and probabilities using the Visual Basic for Applications (VBA) in Excel. Ms. Lambert completed development of the PC-based GUI to display the 5- and 10-minute peak wind speed climatologies and probabilities. She used Visual Basic for Applications in Microsoft® Excel 2002 (hereafter Excel) to develop the tool, which consists of separate input and output GUIs.

Input GUI

The GUI that prompts the user for input needed to retrieve data for output was completed during the quarter and is shown in Figure 1. The input GUI has separate pages for climatology and probability analyses, with tabs at the top for the user to select which analysis is desired. The page for input to retrieve climatology data is on the left and the page for input to retrieve probability data is on the right in Figure 1. For climatology data, the user first chooses the peak speed time interval. The 5-minute peak speed climatologies for the SLF towers (Towers 511, 512, and 513) and Tower 313 were calculated in Phase I. The 10-minute peak wind climatologies for the SLF towers were calculated in a previous quarter (AMU Quarterly Report Fourth Quarter FY-02). After choosing the peak speed time interval of interest, the user chooses the tower and month of interest from the appropriate drop-down lists. The final step is to choose one of the three stratifications and the desired hour and/or direction sector in the associated drop-down box(es). After all choices are made, the user will click on the Get Climatology command button and an output GUI with the retrieved information will be displayed.

The inputs are the same on the probability page, except that the user chooses the empirical or modeled distribution of the time interval/tower/month combination of interest instead of an hourly and/or directional stratification. The user must then select the 5-minute average wind speed of interest, most likely the currently observed or forecast value. The range of values in the empirical and theoretical drop-down lists change according to the choices made for time interval, tower, and month. The Get Probabilities command button will display an output GUI with a range of peak speeds associated with the input average speed and their probabilities of occurrence.
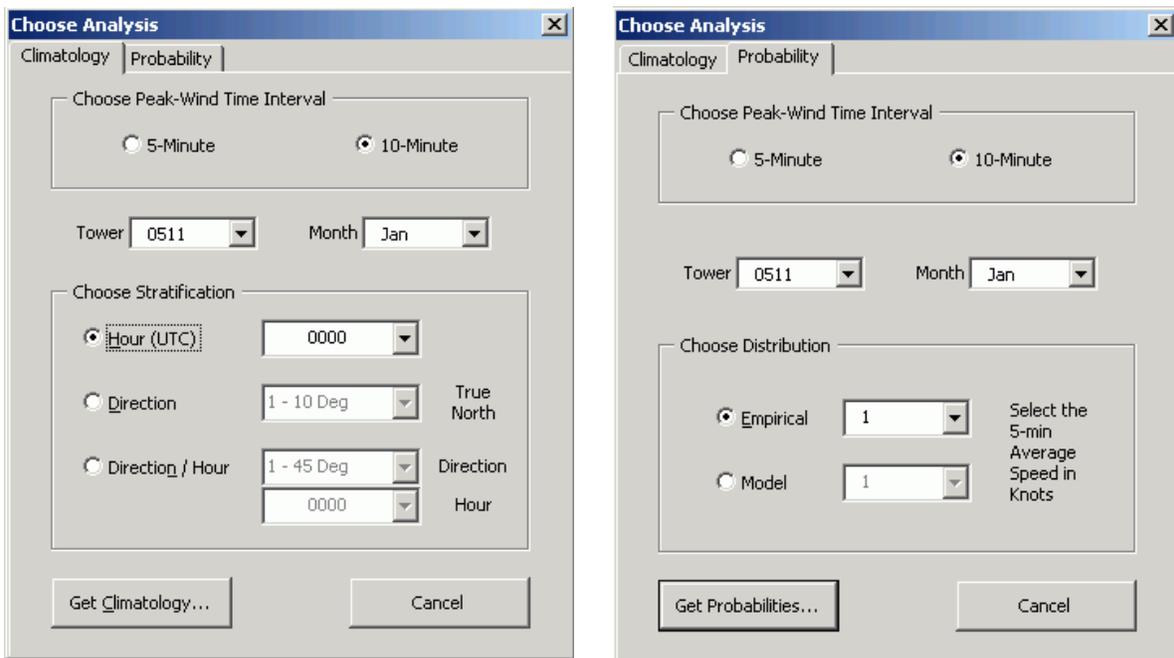

Figure 1. The two input GUI pages used to retrieve climatological or probability of occurrence data. The left panel inputs the information needed to retrieve the climatology data, and the right panel inputs the information needed to retrieve the probability data.

Climatology Output GUI

Once the Get Climatology button is clicked, one of three GUIs is displayed depending on the choice of stratification in the input GUI. The GUI in Figure 2 is the result of choosing the hourly climatology. At the top, the user's choice of peak wind time interval, tower, and month are displayed along with the height of the sensor. In the Stratification area, the user's choice of hour is displayed, with the label 'Hour (UTC)' activated to show that the choice from the input GUI was for the hourly stratification. The label 'Direction' and its associated text box are de-activated and set to light gray so there is no confusion to the user which climatology is being displayed. The climatolologies of interest are displayed in the Wind Statistics section. This includes the mean, standard deviation, and number of observations for the peak and average wind speeds. Next to this section is the Choose Another Analysis button that is used to close the output GUI and allow the user to choose another analysis from the input GUI. The notice at the bottom reminds users that the values displayed are calculated from historical data, not currently observed data, and should not be used as an absolute forecast for future winds.

The directional climatology GUI is not shown here, but is identical to the GUI in Figure 2, with one exception. The user's choice of direction bin is displayed in the Stratification area with the label 'Direction' activated to show that the choice from the input GUI was for the directional stratification. The label 'Hour (UTC)' and its associated text box are de-activated and set to light gray.

Figure 2.   Output GUI for the hourly climatology.   The peak speed time interval, tower number, sensor height, month, and hour of the climatology are displayed in the top half.   The mean, standard deviation, and number of observations are shown for the peak and 5-minute average winds. The Choose Another Analysis button closes the GUI. The notice reminds the user that the data used are historical and not based on current observations.

The GUI in Figure 3 is the result of choosing the directional/hourly climatology. In the Stratification box, both the hour and direction labels and text boxes are activated to show that the choice from the input GUI was for the directional/hourly stratification. The text boxes contain the choice for hour and direction bin. The climatolologies displayed in the 'Wind Statistics' section include the same statistics as for the other two GUIs, except that the number of observations is replaced by the percent of total observations in the hour. Since the total number of observations from a particular direction sector can vary for any hour, displaying the number of observations did not provide enough information about whether wind from a certain direction was more or less common for a particular hour. If all observations in a particular hour were evenly divided between all eight sectors, the value in this box would be 12.5% for every sector. Values larger or smaller than this would show forecasters whether winds from a particular sector were more or less prevalent for a certain hour.
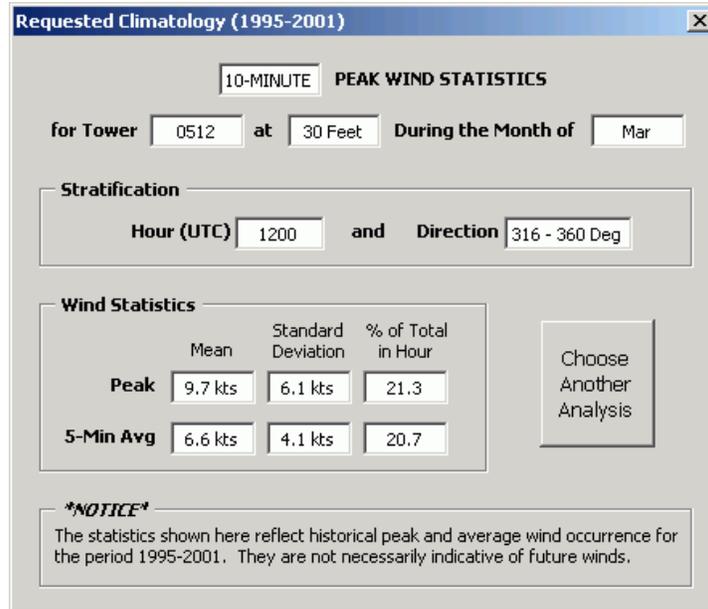

Figure 3. Output GUI for the directional/hourly climatology. The peak speed time interval, tower number, sensor height, month, hour, and direction bin of the climatology are displayed in the top half. The mean, standard deviation, and percent of observations in the hour are shown for the peak and 5-minute average winds. The Choose Another Analysis button closes the GUI. The notice reminds the user that the data used are historical and not based on current observations.

Probability Output GUI

Once the Get Probabilities button is clicked, the GUI in Figure 4 is displayed. The first line displays the user's choice of empirical or modeled distribution and the peak wind time interval. The second line shows the choice of tower and month along with the height of the sensor. The third line shows the choice of 5-minute average wind speed. The probabilities of interest are displayed in the 'Peaks and Probabilities' section. This section contains three rows, each containing 12 text boxes. The first row contains the first 12 values in the distribution of peak speeds associated with the 5-minute average speed (10 knots in Figure 4). If there are less than 12 values in the range, N/As are displayed in the boxes after the last value in the range. Each box in the second row shows the probability, in percent, of meeting or exceeding the peak speed in the box directly above it. The probability values are rounded to the nearest whole number. The last row contains the values of the probability density function (PDF) in percent for each peak speed in the range. This shows the user how often a particular peak speed was observed given the specific 5-minute average speed. In Figure 4, a peak speed of 15 knots has the highest probability of occurrence at 24%, and the probability of meeting or exceeding 15 knots is 78%. To the right of the notice is the 'Retrieve Another Probability Range' button that is used to close the GUI and allow the user to choose another analysis from the input GUI.
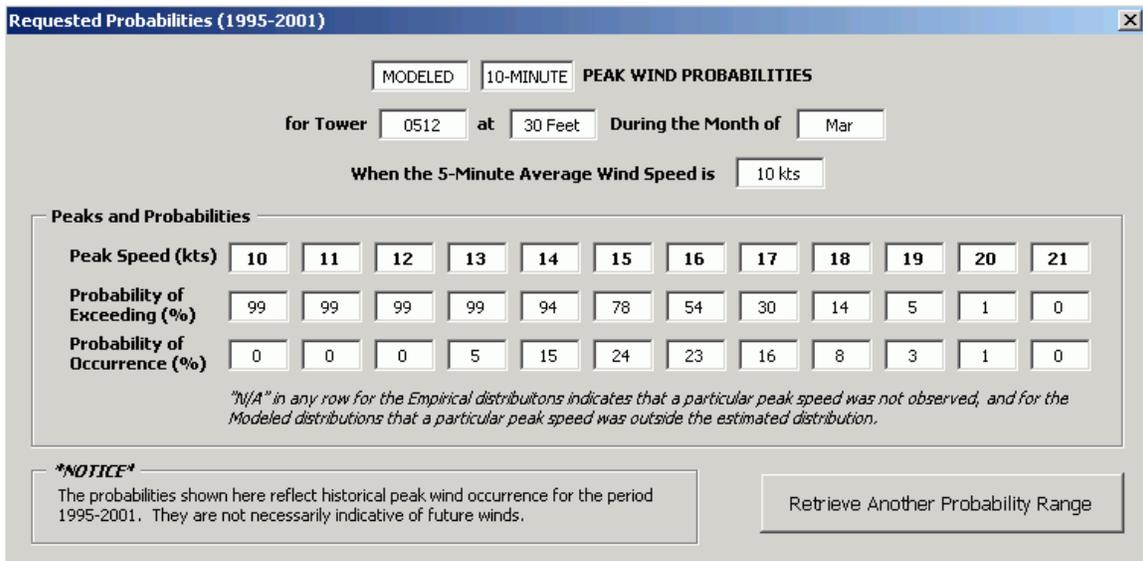
4

Figure 4. Output GUI for the probabilities. The distribution type, peak speed time interval, tower number, sensor height, month, and 5-minute average wind speed are displayed in the top half. The first 12 values in the peak speed distribution and their probabilities of being met or exceeded and probability of occurrence values are shown in the Peaks and Probabilities section. The Retrieve Another Probability Range button closes the GUI. The notice reminds the user that the data used are historical and not based on current observations.

The reason for displaying the first 12 values in the distribution range should be noted here. It is the result of two issues. The first is the inability of the software to be flexible in the number of text boxes displayed in the GUI. To the extent of the programmer's knowledge, the number of boxes must be fixed. The number of boxes is the result of a FR that defines a violation when the peak speed is 10 or more knots greater than the average speed. Displaying the first 12 values in the range will ensure that the probabilities for the peak speeds in question will be displayed. Using this particular FR in Figure 4, a violation would occur if the peak speed reached 20 knots or more. The values for 20 and 21 knots are displayed, which is enough to help SMG forecasters evaluate this FR.

Products and Final Report

The GUIs shown here are the final result of consultations between Ms. Lambert and forecasters at SMG. They were given the GUI algorithm to test and make suggestions for modifications, all of which were incorporated. This ensured that the end product would be easy to use and produce useful information in a readable format. The final form of this product was delivered to SMG and is in operational use. A first draft of the final report was completed and is currently undergoing an internal AMU review.

For more information on this work, contact Ms. Lambert at 321-853-8130 or lambert.winifred@ensco.com.

INSTRUMENTATION AND MEASUREMENT

I&M AND RSA SUPPORT (DR. MANOBIANCO AND MR. WHEELER)

Mr. Wheeler participated in several meetings and teleconferences that addressed AMU hardware/software requirements and maintenance responsibilities. He also reviewed and provided comments on AMU console layout submitted by Lockheed Martin and provided sizes and power requirements of all government furnished equipment.

Table 1. AMU hours used in support of the I&M and RSA task in the Second Quarter of FY 2003 and total hours since July 1996.	
Quarterly Task Support (hours)	*Total Task Support (hours)*
26.5	426.5

EXTEND AMPS MOISTURE PROFILES (DR. SHORT AND MR. WHEELER)

The 45 WS utilizes vertical profiles of humidity and temperature from balloon-borne rawinsonde observations (RAOBs) to assess atmospheric stability and the potential for thunderstorm activity. Operational RAOBs from the Meteorological Sounding System (MSS) were replaced by the Low Resolution Flight Element (LRFE) of the Automated Meteorological Profiling System (AMPS) at the balloon facility (XMR) on Cape Canaveral Air Force Station (CCAFS). Testing of the AMPS LRFE (hereafter AMPS) and earlier comparisons with MSS revealed significant differences in relative humidity (RH) between the two systems (Leahy 2002; Short and Wheeler 2002). Because local experience and thunderstorm forecast rules of thumb are based on a long history of stability indices computed from MSS RAOBs, and because the vertical profile of RH is a sensitive indicator of atmospheric stability, it is important that forecasters become familiar with any changes in humidity data that accompany the transition to AMPS RAOBs. The AMU was tasked to examine the RH differences in detail to evaluate the impact of the humidity differences on the diagnosis of atmospheric stability and thunderstorm indices.

A special data collection campaign was conducted at XMR during July and August 2002, resulting in 20 pairs of humidity and temperature profiles from balloon flights that carried both AMPS and MSS sensors. This warm-season campaign was designed to supplement the cool-season campaign that had been carried out earlier in the year and reported in Short and Wheeler (2002). For the present task extension, Dr. Short and Mr. Wheeler have performed a study of the 20 warm-season dual-sensor profiles and determined that the humidity differences seen during the cool season also occurred in the warm season. Dr. Short also evaluated the impact of the observed humidity differences on thunderstorm forecasting indices used operationally by the 45 WS, SMG, and the National Weather Service Office at Melbourne, FL (NWS MLB). In the previous quarterly report (AMU Quarterly Report First Quarter FY-03), Dr. Short and Mr. Wheeler reported that atmospheric stability indices computed from AMPS and MSS dual-sensor profiles of temperature and humidity, which were taken during July and August 2002, were statistically indistinguishable.

Spectral Analysis of AMPS RH Sensor Response

An additional test of the AMPS RH sensor response time was conducted via a spectral analysis of RH profiles obtained during ascent and descent of the LRFE. Characteristics of interest were the instrument response time, which can smooth out valid small-scale variability, and instrument noise that can introduce artificial small-scale variability. The analysis was confined to altitudes below 30 000 ft where RH variations affect assessments of atmospheric stability. During standard operations, Computer Sciences Raytheon personnel at the CCAFS balloon facility process the AMPS LRFE data for the ascent portion of the flight. The AMU requested that data processing be continued during descent for several flights for the spectral analysis presented below.

During a typical up-down flight, the AMPS LRFE containing the RH sensor is carried aloft by a standard meteorological balloon from the warm, humid lower troposphere, through the cold (-80°C), dry tropopause within 45 minutes. After another 45 minutes of ascent into the dry stratosphere, it reaches a level where the atmospheric pressure is 1/100 of that at the surface. At that point, near an altitude of 100 000 ft, the balloon bursts and the LRFE sensor package falls back to the surface in about 40 minutes with descent slowed by a small parachute. During descent the sensor encounters the warm, moist, high pressure layers at the end of its flight, averaging about 1.5 times the ascent rate in the mid-to lower-troposphere. Throughout ascent and descent the LRFE drifts with the atmospheric currents. Due to the difference in ascent and descent rates, and the time the balloon drifts with the environmental winds, the sensor package typically lands tens of nautical miles from its release point. As a result, a precise agreement in RH profiles between the ascent and descent portions of the flight cannot be expected. Nevertheless, aspects of sensor performance related to instrument noise and response time can be evaluated under these markedly differing conditions by using spectral analysis techniques.

Because small-scale variability in the atmosphere is strongly affected by turbulent processes, the power spectral density (PSD) of atmospheric characteristics can be expected to follow a power-law dependence (e.g. Merceret 2000). A distinct deviation from a power-law, such as a high frequency plateau, would be consistent with instrument noise. Effects of a slow instrument response time would be manifest by a cut-off in the PSD at frequencies higher than the response time.

Figure 5 shows the wavenumber (number of cycles per ft) versus the average PSD for the ascent and descent segments from 11 June 2002 and 25 September 2002 within the troposphere. Each data segment was composed of 64 1-second point values, representing ~ 1184 ft in altitude during ascent and ~ 1776 ft during descent. These two scales establish the minimum wavenumbers in the analysis at 1/(1184 ft) and 1/(1776 ft), respectively, for the ascent and descent portions. Forty-six segments were available on ascent and 30 segments were available on descent. Spectra were computed using a fast-Fourier-transform (FFT) algorithm in the S-PLUS® software package (Insightful Corporation 2000). Both spectra follow a power law with a coefficient, or slope, near –2.4. This is remarkably close to the slope found by Merceret (2000) for vertical profiles of horizontal wind speed from the 50-MHz Doppler wind profiler on Kennedy Space Center. The spectra do not show indications of an instrument noise plateau, nor do they suggest the effects of a slow instrument response time. The close agreement of the spectra obtained during ascent and descent indicate that the AMPS RH sensor performed consistently under markedly differing conditions.

Power Spectra versus Wavenumber
AMPS RH Profiles: 11 June and 25 September, 2002

Descent (dashed)
$y = 1.555E\text{-}07x^{-2.44}$
$R^2 = 0.96$

Ascent (solid)
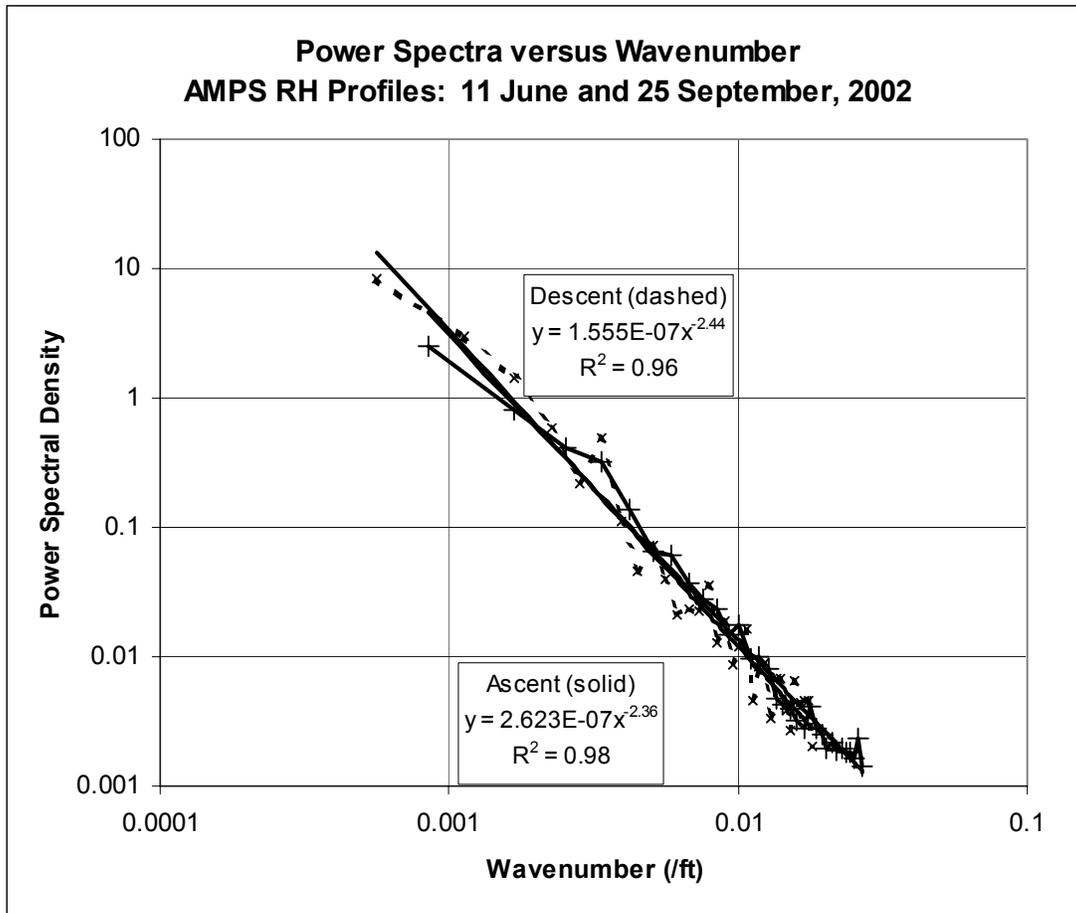$y = 2.623E\text{-}07x^{-2.36}$
$R^2 = 0.98$

Figure 5. Vertical wavenumber versus average power spectral density of RH from AMPS flights on 11 June and 25 September 2002. The ascent portion is indicated by solid line connecting + symbols. The descent portion is indicated by dashed lines. Solid straight lines represent a least-square power-law fit to the data points. Coefficients are shown within the solid boxes. The squares of the correlation coefficients (R) are also shown.

Summary and Conclusions

AMPS, the current operational system for determining vertical profiles of RH, temperature, pressure and wind using balloon-borne sensors and Global Positioning System (GPS) tracking, has replaced the MSS, which uses balloon-borne sensors and radar-tracking. The observed vertical profile of RH from such systems is critically important to the 45 WS, SMG, and NWS MLB for assessing atmospheric stability and the potential for thunderstorm activity. However, the local climatology and severe weather forecasting rules have been influenced by more than 20 years of experience with stability indices derived from MSS. The presence of systematic differences in RH between AMPS and MSS found in preliminary testing necessitated a detailed examination of the impact of such differences on stability indices used in severe weather forecasts. The AMU was tasked to evaluate RH differences between AMPS and MSS from a database of 26 dual-sensor profiles obtained during January, February, and April 2002. The AMU reported a systematic pattern of RH differences that caused the atmosphere to appear slightly less stable when diagnosed from AMPS as compared to MSS (Short and Wheeler 2002). The AMU made interim operation recommendations for adjusting AMPS stability indices, based on projections from the analysis of cool-season data to the warm-season (May through September).

Additional dual-sensor profiles were obtained during the warm-season and the AMU was further tasked to analyze them. The analysis of 20 dual-sensor profiles from the warm-season (July and August) confirmed the basic pattern of RH differences found in the cool-season data (Short and Wheeler 2002): AMPS RH ~ 5% higher when MSS RH is > 70%, and ~ 10% lower when MSS RH is < 30%. As a result, the atmosphere would appear less stable when diagnosed with an AMPS RAOB than with an MSS RAOB, assuming that their temperature profiles were equal. However, the AMPS and MSS stability indices computed from the warm-season dual-sensor profiles were found to be statistically indistinguishable. This apparent paradox was resolved by evidence of a weak systematic temperature difference between AMPS and MSS that counteracts effects of the RH difference on stability indices. As a result, the AMU has rescinded its earlier interim operational recommendations based on the cool-season data and has proposed that AMPS soundings and stability products be used without modification.

For more information on this work, contact Dr. Short at 321-853-8105 or short.david@ensco.com, or Mr. Wheeler at 321-853-8205 or wheeler.mark@ensco.com.

MiniSODAR Evaluation (Dr. Short and Mr. Wheeler)

The Doppler miniSODAR™ System (DmSS) is an acoustic wind profiler from AeroVironment, Inc., that provides vertical profiles of wind speed and direction with high temporal and spatial resolution. The DmSS in this evaluation is a model 4000 system configured to provide 30-second wind estimates at 23 vertical levels from 49.2 to 410.1 ft (15 to 125 m) every 5 m (16.4 ft). It is a phased array system with 32 speakers that are used to form 3 beams for measuring orthogonal components of the wind field, 2 horizontal and 1 vertical. The Boeing Company installed a DmSS at Space Launch Complex 37 (SLC-37) as a substitute for a tall wind tower. It will be used to evaluate the launch pad winds for the new Evolved ELV during ground operations and to evaluate LCC during launch operations. In order to make critical Go/No Go launch decisions the 45 WS Launch Weather Officers (LWOs) and forecasters need to know the quality and reliability of DmSS data. The AMU was tasked to perform an objective comparison between the DmSS wind observations near SLC-37 and those from the nearest tall (≥ 204 ft) wind tower.

Comparison of Average Wind Speed Profiles

The tall wind tower nearest to SLC-37 is Tower 0006, at a distance of 0.95 n mi to the south-southeast. Tower 0006 has wind speed and direction instruments at 4 levels: 12, 54, 162 and 204 ft. Tower 0108 is closer, a distance of 0.6 n mi to the NW, but its wind sensors are only at 12 and 54 ft, the latter being close to the lowest level from the DmSS at 49.2 ft. In addition to these nearby wind towers there is a sonic anemometer at the DmSS site mounted on a 33 ft (10 m) pole, about 100 ft SW of the DmSS. Wind data from the sonic anemometer is integrated into the DmSS data stream and reported at the 33-ft level.

On 9 January 2003, the DmSS was reconfigured to provide wind estimates every 30 seconds instead of 1 minute to provide the LWO with rapid updates of the average wind and wind gusts during a launch window. Figure 6 shows a comparison of average wind speed profiles for the 20-day interval from 10-29 January 2003 following the reconfiguration. Data are from the DmSS, Towers 0006 and 0108, and the sonic anemometer at the DmSS site. There is good agreement between the DmSS and Tower 0006 above 150 ft. At 54 ft there are clear indications of an under-estimate by the DmSS compared to the other instruments. One possible reason for low wind speed estimates from the DmSS would be contamination by nearby stationary structures. Acoustic echoes returned from stationary structures will have a zero-Doppler-velocity. When the effects of these zero velocities are averaged into a final value the result is an under-estimate in wind speed. Effects of this type of contamination appear to be negligible above an altitude of about 125 ft. Although there are no wind tower data between 54 ft and 162 ft, the average wind speed profile for a 20-day time period would be expected to vary smoothly with height, as roughly indicated by linear interpolation between the levels in Figure 6 (dashed line). The AMU will investigate logarithmic interpolation in the future as a possible method to estimate the average wind profile between wind tower levels.
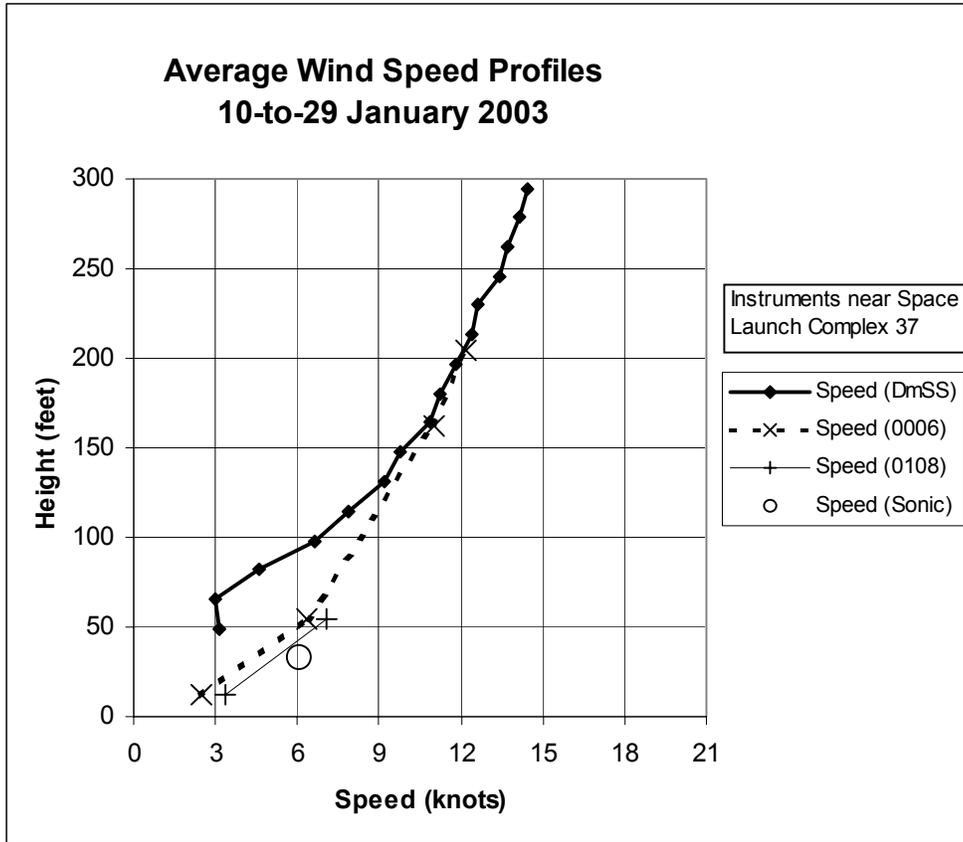
Figure 6.   Vertical profiles of average wind speed from the DmSS (heavy solid), Tower 0006 (dashed), and Tower 0108 (light solid) for the period 10-29 January 2003.   The average wind speed from the sonic anemometer is indicated by a circle.

Figure 7 shows vertical profiles of peak wind speeds from the DmSS, Towers 0006 and 0108, and the sonic anemometer.   The DmSS and sonic anemometer report a wind gust speed every 30 seconds, whereas the data archive from the tower instruments has a peak wind speed every 5 minutes, based on 1-second data.   Peak and gust are assumed here to be synonymous, varying only in the nomenclature used by the data providers, despite the technical differences in the wind measuring equipment.   Figure 7 indicates that the average DmSS gust speeds are less than the other instruments below about 125 ft and greater above 125 ft.   The reason for under-estimates below 125 ft is most likely to be related to the contamination by stationary structures mentioned above.   The differences above 125 ft are not understood at this time and will be the subject of further investigation.

Average Peak and Gust Speed Profiles
10-to-29 January 2003

Instruments near Space Launch Complex 37

Legend:
— Gust (DmSS)
— ×— Peak (0006)
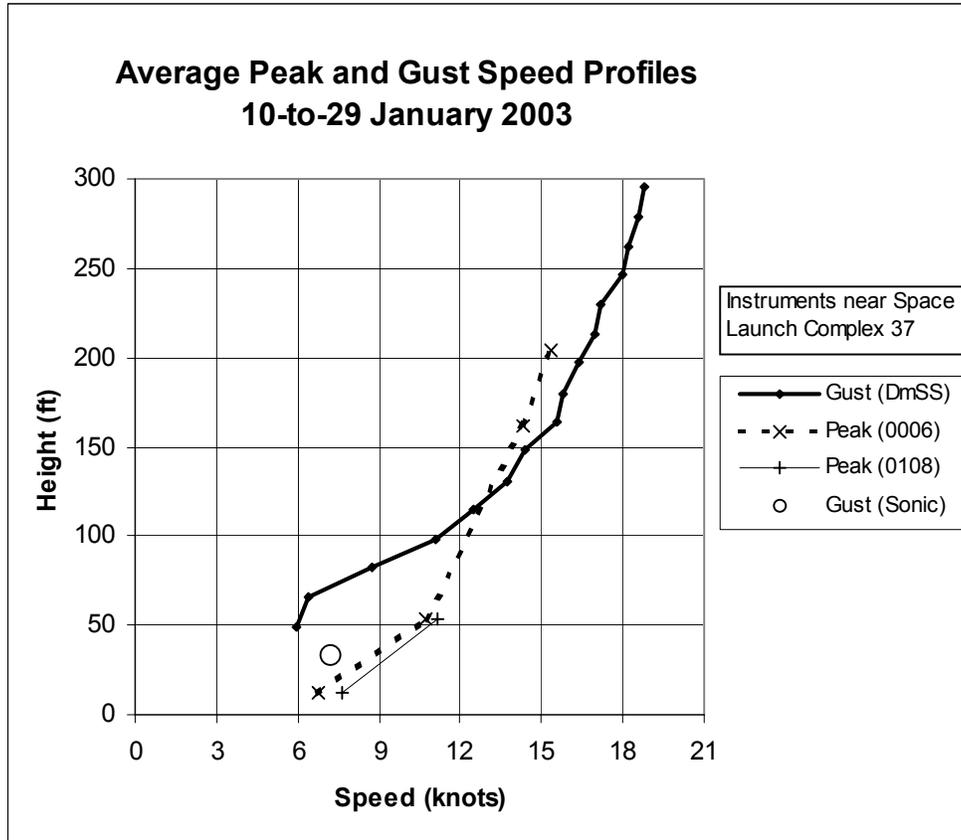—+— Peak (0108)
○ Gust (Sonic)

Figure 7. Vertical profiles of the average peak wind speed from Towers 0006 (dashed) and 0108 (thin solid), the average gust speed from the DmSS (heavy solid), and the average gust speed from the sonic anemometer (o) at the DmSS site for the period 10-29 January 2003.

10 March 2003 Data Analysis

Dr. Short developed software to compute 5-minute average DmSS wind data in order to facilitate direct comparisons with wind tower data. For each 5-minute interval, the DmSS supplies 10 values of 30-second average wind speed/direction and wind gust speed/direction. Vector averaging is applied to the average wind speed and direction data, whereas the maximum gust speed of the 10 values, and its associated direction, is used for each 5-minute interval of DmSS data. Figure 8 shows the 24-hour time series for 10 March 2003 of 5-minute peak wind speeds from the 54 ft level of Tower 0108 and from the 49.2 ft (15 m) level of the DmSS. The DmSS and wind tower agree reasonably well between 1400-to-2100 UTC, with a marked tendency for the DmSS to under-estimate otherwise. The increase in DmSS winds after 1200 UTC occurred near sunrise at 1138 UTC, whereas the decrease in DmSS winds after 2100 UTC occurred near sunset at 2328 UTC. These data indicate that the low-level atmospheric stability may affect DmSS performance at low altitudes.
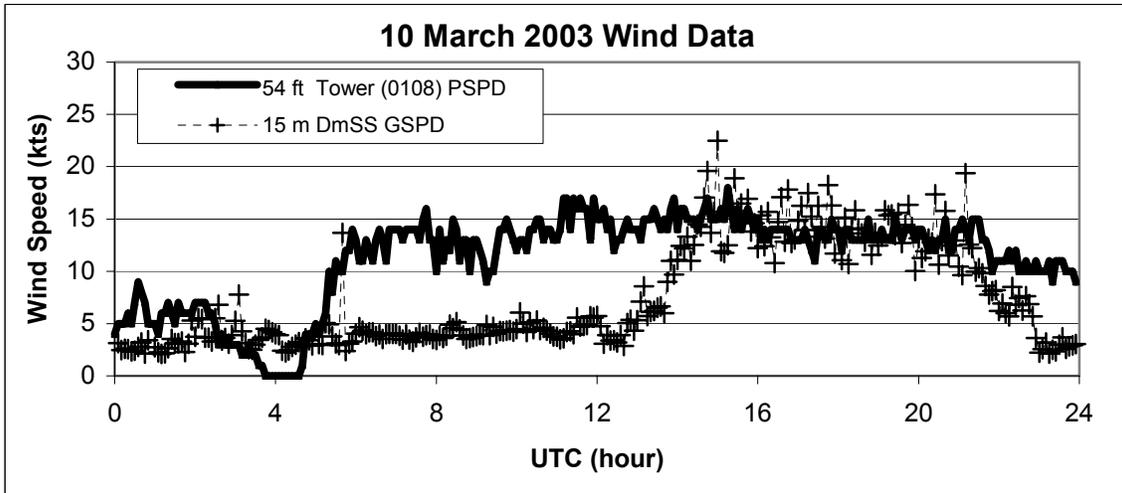
Figure 8.   The 10 March 2003 24-hour time series of 5-minute peak wind speeds from the 54-ft level of Tower 0108 (heavy solid line) and the 49.2 ft (15 m) level of the DmSS (+). Sunrise occurred at 1138 UTC and sunset occurred at 2328 UTC.

Figure 9 shows the 10 March 2003 24-hour time series of 5-minute peak wind speeds from the 162 ft level of Tower 0006 and from the 164 ft (50 m) level of the DmSS. The DmSS and wind tower agree reasonably well throughout the day, with a general tendency for the DmSS gust speeds to be higher than the peak wind speeds from the tower. This latter tendency is consistent with the average profiles shown in Figure 7 and is likely due to a combination of two or more factors: 1) A lack of contamination by stationary structures at the higher levels, and 2) Some presently unknown reason(s) for the average DmSS gust speed to exceed the average wind tower peak speed at levels above 125 ft. Further investigation into the nature of these differences will be undertaken during the next quarter.

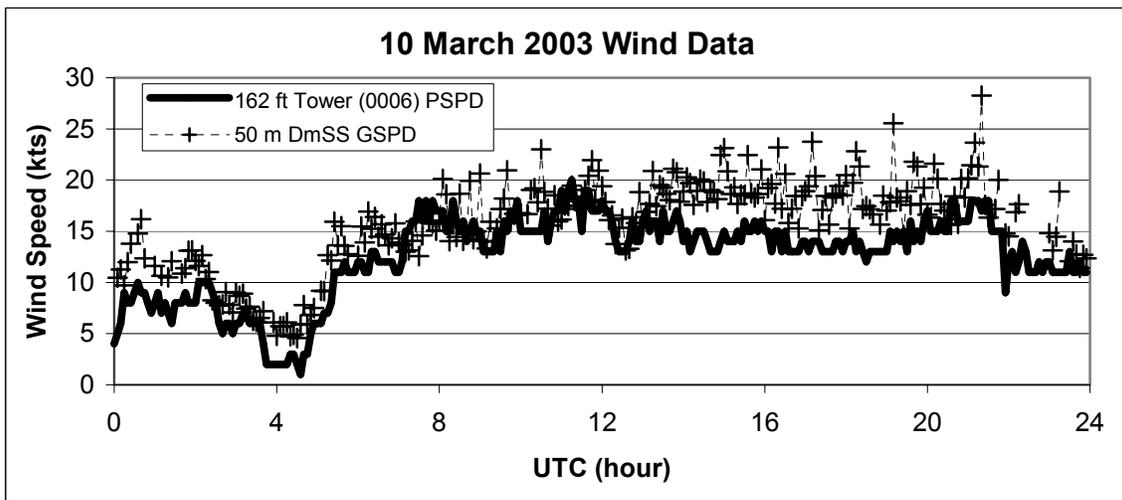Figure 9.   The 10 March 2003 24-hour time series of 5-minute peak wind speeds from the 162-ft level of Tower 0006 (heavy solid line) and the 164 ft (50 m) level of the DmSS (+). Sunrise occurred at 1138 UTC and sunset occurred at 2328 UTC.

For more information on this work, contact Dr. Short at 321-853-8105 or short.david@ensco.com, or Mr. Wheeler at 321-853-8205 or wheeler.mark@ensco.com.

MESOSCALE MODELING

LOCAL DATA INTEGRATION SYSTEM OPTIMIZATION AND TRAINING EXTENSION (MR. CASE)

Both SMG and NWS MLB are running a real-time version of the Advanced Regional Prediction System (ARPS) Data Analysis System (ADAS) to integrate a wide variety of national- and local-scale observational data (Case et al. 2002). While the analyses have become more robust through the inclusion of additional local data sets and the modification of several adaptable parameters, further improvements are desired prior to configuring and initializing the ARPS model with ADAS analyses in future AMU tasks. In addition, limited training would facilitate the transfer of the ARPS/ADAS software configuration and maintenance responsibilities to the NWS MLB and SMG. As a result, the AMU is tasked to improve the real-time data ingest by improving the background fields, expanding the analysis domain, including additional data sets, and modifying the ingestion of selected data sets. Finally, the AMU will provide limited training to NWS MLB and SMG forecasters regarding the maintenance of data-ingest programs and adjustments to the local ADAS configuration.

The AMU completed the implementation of a single expanded analysis grid at NWS MLB and developed a training manual for both SMG and NWS MLB. The new grid currently runs operationally at NWS MLB, and the analysis graphical output can be viewed in real time at the web site

http://www.srh.noaa.gov/mlb/ldis/4km/ldis_currentwx_temp.html.

The training manual includes a detailed description of the program and scripts used to run the ADAS cycle and graphics generation, as well as a directory tree structure to guide users through the file organization. This training document was delivered in both hard and soft copy format, along with the final task memorandum.

For more information on this work, contact Mr. Case at 321-853-8264 or case.jonathan@ensco.com.

VERIFICATION OF NUMERICAL WEATHER PREDICTION MODELS (DR. MANOBIANCO AND MR. CASE)

This project is an option-hours task funded by Kennedy Space Center (KSC) under the Center Director's Discretionary Fund. It is a joint effort between the KSC Engineering Support Contractor, Dynacs, Inc., and the AMU. A key to improving mesoscale numerical weather prediction (NWP) models is the ability to evaluate the performance of high-resolution model configurations. Traditional objective evaluation methodologies developed for large-scale models cannot verify phenomenological forecasts from mesoscale models, and subjective manual alternatives are lengthy and expensive. New objective quantitative techniques are required for evaluating high-resolution, mesoscale NWP models. Therefore, in coordination with personnel from Dynacs, Inc., the AMU was tasked to develop advanced techniques for the objective evaluation of mesoscale NWP models currently employed or under development for Range use. Archived Regional Atmospheric Modeling System (RAMS) forecasts and KSC/CCAFS wind-tower observations were used to develop the objective verification algorithms for the sea-breeze phenomenon. The verification of sea breezes was chosen because this phenomenon is predicted well by RAMS and the sea-breeze boundary is often nearly linear and narrow in width, making the geometry simple.

Personnel from ASRC Aerospace (formerly Dynacs, Inc.) and the AMU completed a final report that was submitted to the KSC Center Director. The report described the automated Contour Error Map (CEM) technique developed for verification of RAMS sea breezes during the months of July and August 2000 and presented summary verification statistics. In addition to the task final report, the AMU added additional data and analysis to validate the CEM algorithm developed by ASRC Aerospace personnel. This report is currently undergoing internal review and will be published as an AMU final report. A manuscript will be drafted from the final report and submitted to an American Meteorological Society (AMS) journal after the AMU final report is published. Finally, a conference paper was written and submitted to the AMS 10th Conference on Mesoscale Processes, and will be presented in Portland, OR in June. The paper presents an analysis of a multi-day sea- and land-breeze event from May 2000, including output from the automated CEM sea-breeze verification algorithm. The following sections, drawn from the conference paper, present the automated CEM sea-breeze verification technique as applied to RAMS forecasts for east-central Florida from 10–13 May 2000.

CEM Technique to Verify Model Sea Breezes

The CEM technique was designed to use 5-minute wind direction data from KSC/CCAFS towers and RAMS forecasts in order to automate and quantify the skill of RAMS in predicting the sea-breeze (SB) phenomenon over the KSC/CCAFS domain. CEM employed a binary wind direction threshold to distinguish between easterly (onshore) and westerly (offshore) wind directions. This method incorporated both spatial and temporal wind data at each grid point of analyzed observed and forecast grids to identify observed and forecast SB transition times. A filtering technique was implemented to identify the correct transition times from offshore to onshore wind flow. To ensure focus on the SB boundary only, an erosion technique was introduced to remove extraneous boundaries not associated with the primary SB front, such as river breezes and precipitation outflow boundaries.

Since the coastline of east-central Florida is approximately oriented along a north-south direction, wind directions between 0° and 180° were considered onshore winds, while 180° to 360° wind directions were defined as offshore. These thresholds could be fine-tuned in the future to more closely match the orientation of the Florida coastline. A histogram of the point-by-point differences in SB transition times between the forecast and observed fields was then generated. A Gaussian function $\hat{h}_k$ was fitted to the CEM histogram data h_k in order to quantify and parameterize the comparison in terms of four parameters:

$\tau \equiv$ mean bias,

$\sigma \equiv$ standard deviation of bias,

$f_O \equiv$ fractional area of only observed SB transition, and

$f_R \equiv$ fractional area of only RAMS SB transition.

The form of the Gaussian histogram function used in this study is given by:

$$\hat{h}_k = \frac{1 - f_O - f_R}{\sigma\sqrt{\pi}} \Delta t \; e^{-(t_k - \tau)^2 / \sigma^2} \tag{1}$$

where t_k is the time corresponding to h_k, the subscript k corresponds to the kth 5-minute bin (the forecast – observed SB transition time difference), and Δt = 5 minutes (the time interval between successive observed and forecast wind fields).

For days with an overlapping observed and forecast SB transition within the grid domain, the Gaussian function fit was performed to produce a set of parameters that describe the quality of the RAMS forecast SB. Days with small mean biases and small standard deviations of the bias indicate more accurate forecasts of the SB transition timing and movement. In addition, the mean wind direction and wind speed were computed on the seaward side of the SB transitions in order to determine the skill of RAMS in predicting the movement of the SB boundary and the representativeness of the post-SB wind environment. Finally, to improve upon the 0–180° wind direction threshold, a time-estimation filter was developed to determine the SB transition times in both the observed and forecast grids. The primary effect of the filter is to identify SB transition times while suppressing the effects of outflow boundaries (convective rainfall).

Image erosion is a common processing technique used to shrink an image object in some predictable way (Gonzalez and Woods 1992). Image erosion was used to suppress the river breeze part of the SB transition time images, using the gradient of the transition times to trigger the erosion process. Due to the terrain around KSC/CCAFS, a river breeze can often develop in advance of the actual SB transition, and move from west to east, opposite of the direction of the SB. By scanning east to west, if a negative gradient was detected (i.e. a boundary moving west to east, which cannot physically be a SB transition), then all SB times to the west of that point were re-coded as "no SB". This simple technique resulted in a reasonable exclusion of areas affected by the river-breeze phenomenon which contaminated the primary SB signal.

Verification of RAMS Forecast Sea Breezes

Figure 10 shows the observed and forecast isopleths of the SB transition time for 10 and 11 May 2000, as determined by the objective CEM method. The observed SB transition times (Fig. 10a) are several hours later than RAMS (Fig. 10b) across much of the analysis domain on 10 May. Meanwhile, the SB transition times compare quite favorably on 11 May between the observed (Fig. 10c) and RAMS isopleths (Fig. 10d). Figure 11 depicts the spatial timing biases as derived from the CEM algorithm for both 10 May (Fig. 11a) and 11 May (Fig. 11b). Clearly, RAMS performed much better on 11 May in predicting the SB onset and movement. Most timing errors on 11 May were less than 1.5 hours in magnitude compared to timing errors of -2.0 to -4.5 hours on 10 May (negative errors indicate early time biases).

Table 1 provides a summary of the CEM Gaussian fit parameter statistics for the verification of the RAMS SB transition times corresponding to each day from 10−13 May. The subjectively-determined ranges of the observed and forecast SB transition times are also shown in columns 6 (Obs Times) and 7 (RAMS Times), respectively, as a means of qualitatively validating the CEM results. These subjective time ranges were determined based on a meteorological analysis of the observed and forecast wind fields in which the presence of a westward-propagating sea-breeze front was determined. Note that if neither a forecast nor observed SB had occurred on a particular day, zeros would appear for both f_O and f_R (no observed only or forecast only SB area). A complete forecast miss or false prediction of a SB on a particular day is represented by a value of one for f_O (forecast failure) or f_R (false alarm prediction).

The RAMS forecasts from 11−13 May had the best skill in predicting the SB occurrence and timing, since those days had the smallest absolute values of the mean bias (τ) and the smallest standard deviation of the bias (σ). Days that have a larger absolute value of τ indicate the greatest domain-wide timing biases in RAMS (e.g. the large negative timing bias from 10 May). The standard deviation of the bias indicates the amount of spatial variation in the timing errors across the KSC/CCAFS domain. A large value of σ indicates a high amount of spatial variation in the SB timing errors.

The observed and RAMS forecast post-SB wind direction and speed averages for 10−13 May are shown in the final four columns of Table 1. The RAMS prediction of the post-SB wind direction was better than the prediction of the post-SB wind speeds. RAMS tended to have a substantially higher post-SB mean wind speed compared to observations, particularly on 10−12 May.
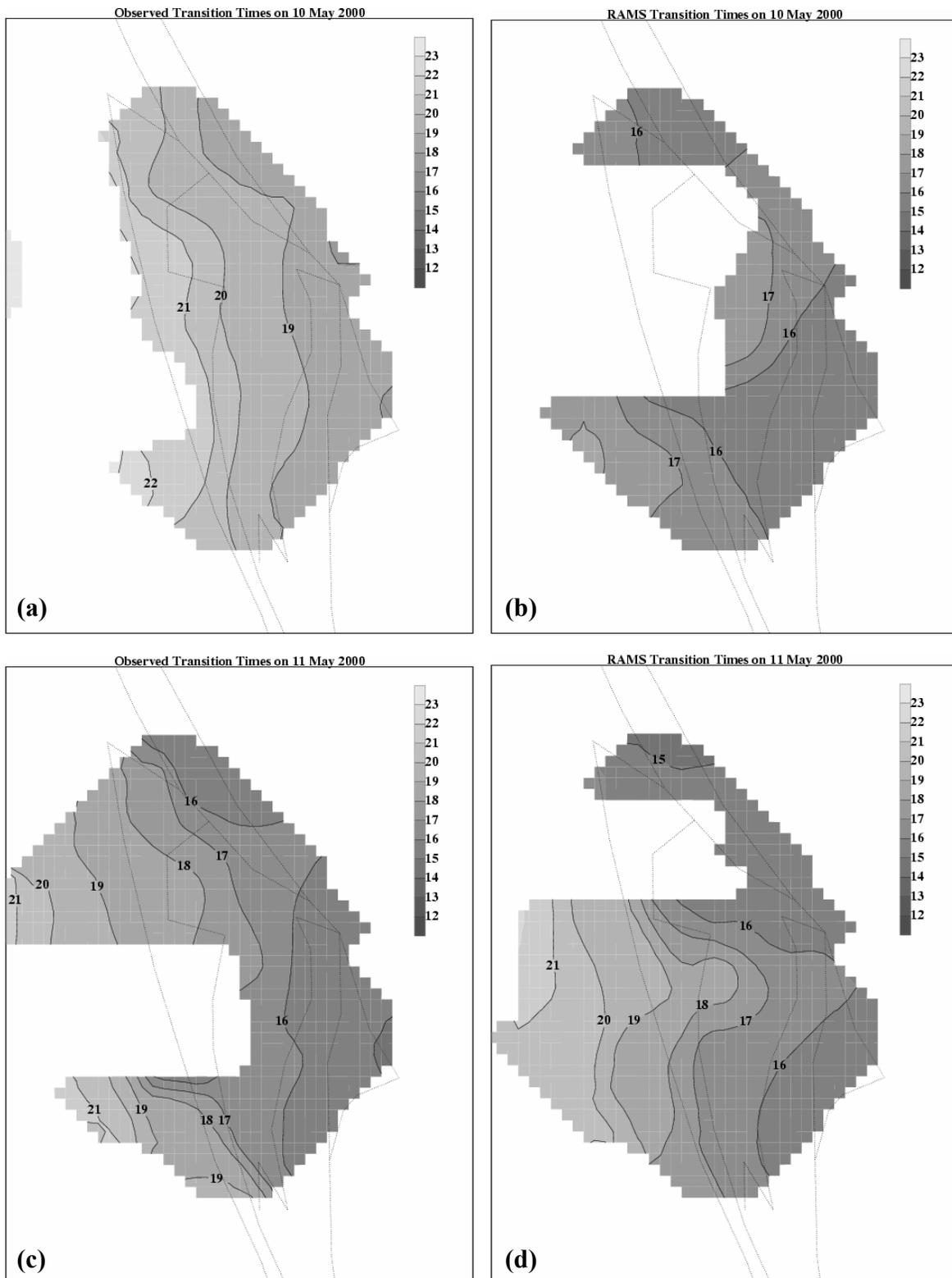
Figure 10. Observed and RAMS forecast isopleths of sea-breeze transition times (in UTC hours) for 10 and 11 May 2000, based on the results of the CEM verification algorithm. Transition times are shown for the (a) 10 May observed winds, (b) 10 May forecast winds, (c) 11 May observed winds, and (d) 11 May forecast winds.
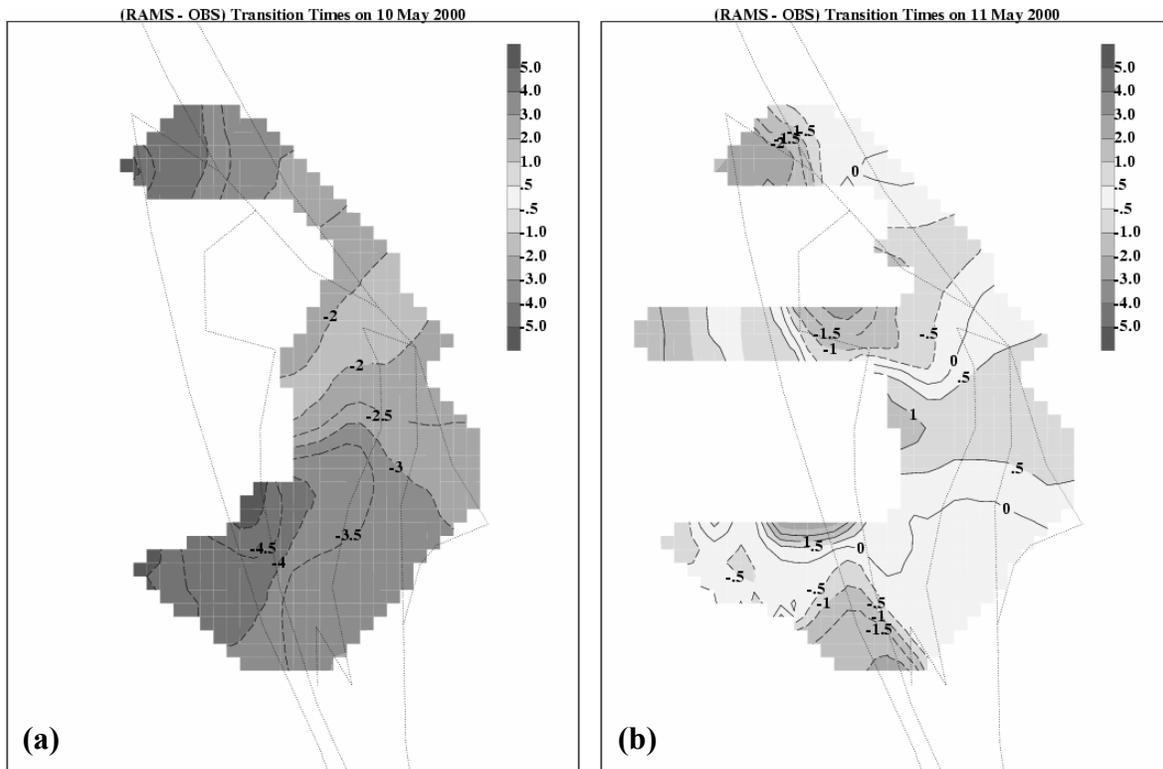
Figure 11.   The differences between the observed and RAMS forecast sea-breeze transition times in hours for (a) 10 May, and (b) 11 May. Negative values indicate an early timing bias by RAMS.

Table 1. Gaussian fit parameters for eroded CEM histograms, subjectively-determined range of observed and RAMS times of the SB transition (in UTC), and the mean post-SB observed and forecast wind directions (WD, degrees) and wind speeds (WS, kt) as calculated in CEM.

Day	τ(h)	σ(h)	f_O (%)	f_R (%)	Obs Times	RAMS Times	Post-SB Obs WD	Post-SB RAMS WD	Post-SB Obs WS	Post-SB RAMS WS
10	-3.1	1.4	31	8	1715 – 2230	1530 – 1815	142°	126°	9 kt	12 kt
11	-0.0	0.9	21	26	1445 – 1945	1515 – 1915	106°	126°	7 kt	12 kt
12	0.0	0.5	8	17	1400 – 1530	1415 – 1530	80°	97°	6 kt	10 kt
13	-0.6	0.5	2	12	1500 – 1730	1500 – 1630	85°	86°	7 kt	8 kt

Summary of CEM Technique Results

The CEM automated model verification method was developed to identify SB transition times in both observed and forecast gridded wind fields. The results of this algorithm compared favorably to subjective analysis and successfully verified the RAMS forecast SB transition zones across the KSC/CCAFS domain.   A phenomenological-based method such as CEM can save a substantial amount of time and resources when verifying mesoscale NWP models. The CEM also helps to improve the quality of verification results by focusing on the phenomenon rather than traditional error statistics, which cannot adequately quantify the utility of mesoscale model forecasts.

17

For more information on this work, contact Mr. Case at 321-853-8264 or case.jonathan@ensco.com.

AMU CHIEF'S TECHNICAL ACTIVITIES (DR. MERCERET)

Dr. Merceret completed an analysis of the effect of radar scan strategies and propagation conditions on the limitations of radar as a tool to accurately assess Lightning LCC. He, Ms. Ward and Mr. Brooks of Dynacs, Inc. conducted an analysis of attenuation recovery time of the WSR-74C radome after wetting by rainfall for the Lightning LCC (LLCC) program. He, Ms. Ward and Mr. Wheeler also completed preparation of daily weather summaries for the LLCC program flight days.

In February and March, Dr. Merceret's primary scientific efforts were directed toward providing data and analyses to assist in the STS-107 debris recovery effort.

AMU OPERATIONS

Mr. Wheeler began work on a 45 WS Option Hours task to analyze wind tower and other data from a severe weather event that occurred near the SLF on 3 March 2003. He submitted the Fiscal Year 2003 AMU equipment and software procurement plans. He also requested quotes from several vendors on AMU hardware requirements, and submitted procurement requests to NASA for renewal of services and hardware purchases.

Ms. Lambert began work on a KSC Option Hours task to evaluate daily rainfall data in support of the STS-107 accident investigation. She also completed modifications to the AMU website to improve the appearance and make it easier to navigate the site.

Dr. Manobianco and Mr. Wheeler attended the 83rd AMS Annual Meeting in Long Beach, CA.

REFERENCES

Case, J. L., J. Manobianco, T. D. Oram, T. Garner, P. F. Blottman, and S. M. Spratt, 2002: Local data integration over east-central Florida using the ARPS Data Analysis System. Wea. Forecasting, **17**, 3-26.

Gonzalez, R. C. and R. E. Woods, 1992: Digital Image Processing. Addison-Wesley Publishing Company, 716 pp.

Insightful Corporation, 2000: *S-PLUS® 6 User's Guide*, Insightful Corp., Seattle, WA, 470 pp.

Lambert, W. C., 2002: Statistical short-range guidance for peak wind speed forecasts on Kennedy Space Center/Cape Canaveral Air Force Station: Phase I Results. NASA Contractor Report CR-2002-211180, Kennedy Space Center, FL, 39 pp. [Available from ENSCO, Inc., 1980 N. Atlantic Ave., Suite 230, Cocoa Beach, FL, 32931.]

Leahy, F., 2002: Analysis of the Automated Meteorological Profiling System Low Resolution Flight Element Thermodynamic data. Raytheon ITSS Memorandum to Stewart Deaton, NASA/MSFC/ED44, May 15 2002, 41 pp.

Merceret, F. J., 2000: The coherence time of midtropospheric features as a function of vertical scale from 300 m to 2 km. *J. Appl. Meteor.*, **39**, 2409-2420.

Short, D. A., and M. M. Wheeler: 2002: AMPS Moisture Profiles. AMU Memorandum, July 2002, 16 pp. [Available from ENSCO, Inc., 1980 N. Atlantic Ave., Suite 230, Cocoa Beach, FL, 32931.]

List of Acronyms

30 SW	30th Space Wing
30 WS	30th Weather Squadron
45 RMS	45th Range Management Squadron
45 OG	45th Operations Group
45 SW	45th Space Wing
45 SW/SE	45th Space Wing/Range Safety
45 WS	45th Weather Squadron
ADAS	ARPS Data Analysis System
AFSPC	Air Force Space Command
AFWA	Air Force Weather Agency
AMPS	Automated Meteorological Profiling System
AMS	American Meteorological Society
AMU	Applied Meteorology Unit
ARPS	Advanced Regional Prediction System
CCAFS	Cape Canaveral Air Force Station
CEM	Contour Error Map
CSR	Computer Sciences Raytheon
DmSS	Doppler miniSODAR System
ELV	Expendable Launch Vehicle
FFT	Fast Fourier Transform
FR	Flight Rule
FSL	Forecast Systems Laboratory
FSU	Florida State University
FY	Fiscal Year
GPS	Global Positioning System
GUI	Graphical User Interface
ITSS	Information Technology and Scientific Services
JSC	Johnson Space Center
KSC	Kennedy Space Center
LCC	Launch Commit Criteria
LLCC	Lightning LCC
LRFE	Low Resolution Flight Element
LWO	Launch Weather Officer
MSFC	Marshall Space Flight Center
MSS	Meteorological Sounding System
NASA	National Aeronautics and Space Administration
NCAR	National Center for Atmospheric Research
NOAA	National Oceanic and Atmospheric Administration
NSSL	National Severe Storms Laboratory
NWP	Numerical Weather Prediction
NWS MLB	National Weather Service in Melbourne, FL
PC	Personal Computer
PDF	Probability Density Function
PSD	Power Spectral Density
RAMS	Regional Atmospheric Modeling System
RAOB	Rawinsonde Observation
RH	Relative Humidity
RSA	Range Standardization and Automation

SB   Sea Breeze
SLC-37   Space Launch Complex 37
SLF   Shuttle Landing Facility
SMC   Space and Missile Center
SMG   Spaceflight Meteorology Group
SRH   NWS Southern Region Headquarters
USAF   United States Air Force
UTC   Universal Coordinated Time
VBA   Visual Basic for Applications
WWW   World Wide Web
XMR   CCAFS 3-letter identifier

Appendix A

<table>
<tr><td colspan="5">AMU Project Schedule
30 April 2003</td></tr>
<tr><td>AMU Projects</td><td>Milestones</td><td>Scheduled Begin Date</td><td>Scheduled End Date</td><td>Notes/Status</td></tr>
<tr><td rowspan="5">Objective Lightning Probability Phase I</td><td>Literature review and data collection/QC</td><td>Feb 03</td><td>Apr 03</td><td>On Schedule</td></tr>
<tr><td>Statistical formulation and method selection</td><td>Apr 03</td><td>May 03</td><td>On Schedule</td></tr>
<tr><td>Equation development, tests with verification data and other forecast methods</td><td>Jun 03</td><td>Nov 03</td><td>On Schedule</td></tr>
<tr><td>Develop operational products</td><td>Nov 03</td><td>Jan 04</td><td>On Schedule</td></tr>
<tr><td>Prepare products, final report for distribution</td><td>Jan 04</td><td>Mar 04</td><td>On Schedule</td></tr>
<tr><td rowspan="3">Extend Statistical Forecast Guidance to the SLF Towers</td><td>Create climatologies / determine theoretical distribution for 10-min peaks</td><td>Sep 02</td><td>Oct 02</td><td>Completed</td></tr>
<tr><td>Develop PC-based tool to display climatologies and probabilities</td><td>Oct 02</td><td>Mar 03</td><td>Completed</td></tr>
<tr><td>Prepare products, final report for distribution</td><td>Mar 03</td><td>May 03</td><td>On Schedule</td></tr>
<tr><td rowspan="3">Extend AMPS Moisture Analysis</td><td>Data collection, data reduction, and QC</td><td>Aug 02</td><td>Sep 02</td><td>Completed</td></tr>
<tr><td>Analysis of humidity differences and impact on thunderstorm forecasting indices</td><td>Sep 02</td><td>Jan 03</td><td>Completed</td></tr>
<tr><td>Memorandum</td><td>Feb 03</td><td>Apr 03</td><td>On Schedule</td></tr>
<tr><td rowspan="3">MiniSODAR Evaluation</td><td>Data collection, data reduction, and QC</td><td>Aug 02</td><td>Jul 03</td><td>On Schedule</td></tr>
<tr><td>Comparative analysis of miniSODAR and nearby wind tower observations</td><td>Sep 02</td><td>Jul 03</td><td>On Schedule</td></tr>
<tr><td>Final Report</td><td>Jul 03</td><td>Sep 03</td><td>On Schedule</td></tr>
<tr><td rowspan="4">KSC-Funded Verification of Mesoscale NWP Models</td><td>Literature review</td><td>Mar 02</td><td>Mar 02</td><td>Completed</td></tr>
<tr><td>Develop objective sea-breeze boundary detection algorithm</td><td>Apr 02</td><td>Aug 02</td><td>Completed</td></tr>
<tr><td>Objective verification of RAMS sea-breeze boundaries</td><td>May 02</td><td>Jan 03</td><td>Completed</td></tr>
<tr><td>Final report/Journal publications</td><td>Jan 03</td><td>Mar 03</td><td>Delayed to do Additional Analysis</td></tr>
</table>

AMU Project Schedule 30 April 2003				
AMU Projects	Milestones	Scheduled Begin Date	Scheduled End Date	Notes/Status
LDIS Optimization and Training Extension	Expand outer analysis grid at NWS MLB	Aug 02	Jan 03	Completed
	Revise data ingest programs	Sep 02	Dec 02	Completed
	Training to SMG and NWS MLB personnel	Oct 02	Mar 03	Completed
	Provide recommendations for implementing new features in ADAS	Oct 02	Jan 03	Completed
	Memorandum	Dec 02	Mar 03	Completed
Subtask 12: ARPS Phase I Configuration of Prototype	Configure source code and scripts to prepare for real-time installation	Jan 03	Mar 03	Completed
	Formal assistance in configuring and installing ARPS at NWS MLB	Apr 03	Apr 03	On Schedule

NOTICE

Mention of a copyrighted, trademarked, or proprietary product, service, or document does not constitute endorsement thereof by the author, ENSCO, Inc., the AMU, the National Aeronautics and Space Administration, or the United States Government. Any such mention is solely for the purpose of fully informing the reader of the resources used to conduct the work reported herein.